Available online at www.sciencedirect.com
ScienceDirect
Catalysis Today 119 (2007) 166–174
CATALYSIS TODAY
www.elsevier.com/locate/cattod

Alumina supported cobalt–palladium catalysts for the reduction of NO by methane in stationary sources

Rui Marques [a], Kaoutar El Kabouss [b], Patrick Da Costa [c,*], Stéphanie Da Costa [c], Franck Delacroix [d], Gérald Djéga-Mariadassou [a]

[a] *Laboratoire de Réactivité de Surface, CNRS UMR 7609, Case 178, Université P. et M. Curie, 4 Place Jussieu, 75252 Paris Cedex 05, France*
[b] *ITODYS, CNRS UMR 7086, Groupe LCMDC, Université Paris 7-Denis Diderot, 2, Place Jussieu, 75251 Paris Cedex 05, France*
[c] *Gaz de France, Direction de la recherche, 361 av. du Président Wilson, B.P. 33, 93211 La Plaine Saint-Denis Cedex, France*
[d] *ADEME, 2 Square La Fayette, 49004 Angers, France*

Abstract

In order to improve a ‘‘Three Function Catalysts Model’’, the present paper deals with alumina based catalysts containing cobalt and palladium for the NO reduction by methane.

The deNO$_x$ temperature window was estimated by adsorption and subsequent desorption of NO in lean conditions. Two NO$_x$ desorption peaks were detected for both catalysts. For Pd(0.63)Co(0.58)/Al$_2$O$_3$, the two desorption peaks appeared at 205 and 423 °C, whereas for Pd(0.14)Co(0.57)/Al$_2$O$_3$, the maxima desorption temperature peaks were at 205 and 487 °C. In addition, NO oxidation was also studied to evaluate the catalyst first function. It was found that, the oxidation begins on Co–Pd/Al$_2$O$_3$ around 250 °C. On Pd(0.63)Co(0.58)/Al$_2$O$_3$, 8% of deNO$_x$ were found in the range of the second NO$_x$ desorption peak temperature (410 °C). During TPSR, C$_x$H$_y$O$_z$ species such as formaldehyde were detected. These oxygenate species are the reactive intermediate for deNO$_x$ by methane.

Keywords: Stationary sources; Methane; deNO$_x$; Three-function model

---

1. Introduction

Emission of nitrogen oxides as a by-product of natural gas high-temperature combustion has been a major environmental concern. The SCR of NO$_x$ by methane is a very attractive technology for decreasing NO$_x$ in the stationary sources, because natural gas (methane) is readily available.

Initially, Li and Armor [1] found that the most active catalysts for NO$_x$ removal by methane in oxygen excess were based on cobalt supported on several zeolites. However they are severely affected by the presence of water vapor [1,2]. More recently bimetallic cobalt and palladium loaded zeolites exhibited much more resistance to water vapor than monometallic Co-zeolites [3–5]. Although they are more resistant, these catalysts deactivate under long-term hydrothermal conditions. Another main obstacle of SCR of NO by methane is the low selectivity of the reaction between NO and O$_2$ [6,7]. This is an important obstacle in the case of Pd, since Pd is very active for the total oxidation of methane [8]. The use of Pd, supported on acidic materials such as zeolites, for the SCR of NO$_x$ by methane, is correlated with the stabilization of the Pd^{2+} ions on acidic materials, which have low activity for methane oxidation [9]. Therefore, other acidic materials have been tested, such as sulphated zirconia and sulphated alumina [10–12].

Supported bimetallic catalysts are very interesting materials because one metal can tune and/or modify the catalytic properties of the other metal. Among bimetallic catalysts, cobalt–palladium is the most interesting bimetallic catalyst. The reason is that when compared to the pure metals, the activity and selectivity are higher for several reactions, including the SCR of NO$_x$ by methane [3–5,13,14]. Over platinum group metal-based catalysts, in a zero valent oxidation state, the mechanism of NO$_x$ reduction is now understood and is well-established in a recent paper of Burch et al. [15]. For other catalytic materials, some mechanisms have been suggested

---

* Corresponding author. Tel.: +33 1 44 27 36 26; fax: +33 1 44 27 60 33.
E-mail address: dacosta@ccr.jussieu.fr (P. Da Costa).

0920-5861/$ – see front matter © 2006 Elsevier B.V. All rights reserved.
doi:10.1016/j.cattod.2006.08.019

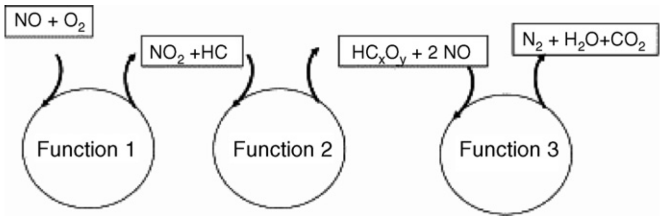

Fig. 1. General model for three-function deNO$_x$ catalyst.

[15,16]. However, up to now the validity of the proposed models is not established for all the catalytic formulations.

More recently, a general three-function model for deNO$_x$ catalysis [17–20] was also proposed for metals in cationic form (Fig. 1). The authors claimed that three functions are necessary for the deNO$_x$ process to occur: (i) oxidation of NO to NO_2; (ii) mild oxidation of methane to alcohol and aldehyde, in the presence of NO_2; (iii) reduction of NO to N_2, assisted by the deep oxidation of the alcohol and aldehyde to CO_2. Simultaneously the active site of the third function is regenerated. Fig. 1 shows the three catalytic cycles which have to turn over simultaneously in order to occur the deNO$_x$ reaction. Cycle 1 provides NO_2 to cycle 2, and cycle 2 delivers the active HC_xO_y oxidised species to cycle 3, in order to proceed to the decomposition–reduction of NO to N_2. The HC_xO_y species are simultaneously transformed to CO_2 and H_2O. The detailed process has already been described on zeolites based catalysts by Berger et al. [21] and on ceria-zirconia based catalysts by Thomas et al. [19]. The interaction between NO_2 and HCl is clearly located in the second catalytic cycle. Baudin et al. have detected RNO$_x$ and shown the decomposition of RNO$_x$ to $C_xH_yO_z$ over a Ir/CeZrO$_2$ catalyst [22]. The dinitrogen is formed in the last cycle and is not linked to any organo-nitro compound. In summary, the catalytic cycles lead to a model of NO reduction assisted by the oxidation of a pre-activated HC_xO_y (lean conditions).

The aim of the present work is to explain the deNO$_x$ catalytic activity of cobalt–palladium catalysts with the three-function model. Moreover, we pretend to clarify and improve this model for SCR deNO$_x$ by methane.

2. Experimental

2.1. Catalysts synthesis

Catalysts were prepared by wet impregnation of crushed and sieved γ-Al_2O_3 ($0.8\ mm < d < 1.2\ mm$) (Procatalyse, specic surface area of 190 $m^2\ g^{-1}$, pore volume of 0.7 $cm^3\ g^{-1}$) with $Pd(NH_3)_4(NO_3)_2$ aqueous solution or cobalt(II) nitrate hexahydrate 99%. The precursor's suspension was maintained under stirring at 333 K for 3 h. After complete removal of water by evaporation under reduced pressure, the catalysts were dried overnight with air at 393 K and calcined with air at 773 K for 2 h. The catalysts preparation procedure is described elsewhere [23]. The as-prepared catalysts are labeled Pd(X)/Al_2O_3 and Co(X)/Al_2O_3, in which X is content of noble metal. For bimetallic catalysts, labeled Pd(X)Co(X)/Al_2O_3, the cobalt is first impregnated on the support. Then, after the treatments presented above, the palladium is added in a successive impregnation. The prepared catalysts are presented in Table 1.

2.2. Characterization of the catalysts

The catalysts were characterized by X-ray diffraction (XRD), transmission electron microscopy (TEM), and UV–vis–near-infrared (NIR). The specific surface area was also measured using a home made apparatus. Elemental analysis was performed by the ‘‘Service Central d'Analyses du CNRS'' in order to determine the cobalt and palladium contents. Powder XRD was carried out on a Siemens model D-500 diffractometer with Cu Kα radiation. High-resolution transmission electron microscopy (HRTEM) was performed to determine the particle size of cobalt and/or palladium particles on alumina and to check their dispersion. HRTEM studies were performed on a JEOL-JEM 100 CXII apparatus associated with a top entry device and operating at 100 kV. EDS analysis was performed with the same apparatus using a LINK AN 10,000 system, connected to a silicon-lithium diode detector, and multichannel analyser. EDS analyses were obtained on large domains of samples (150 nm × 200 nm to 400 nm × 533 nm). Diffuse reflectance spectra were recorded at room temperature between 190 and 2500 nm on a Varian Cary 5E spectrometer equipped with a double monochromator and an integrating sphere coated with polytetrafluoroethylene (PTFE). PTFE was the reference.

2.3. Catalytic measurements

The catalytic reaction was performed with the following reactants: 150 ppm NO, 7 vol.% O_2, 0 vol.% CO_2, 1500 ppm CH_4, 0 vol.% H_2O in Ar as balance. Concerning nitrogen oxide, methane and oxygen, this reaction mixture is representative of the concentrations present in the exhaust gases of combined heat powers (CHP).

The NO mixture was supplied by Air Liquide as 1 vol.% NO, and 99 vol.% Ar (<10 ppm other gases). The O_2 mixture contained 100 vol.% O_2 (Air Liquide). The CH_4 mixture contained 5 vol.% CH_4, and 95 vol.% Ar (Air Liquide). The total gas flow was maintained at 0.25 L min^{-1} NTP. Each gas mixture was metered using calibrated electronic mass flow controllers (Brooks, Model 5850E). Taking a catalyst density of about 0.7 g/cm^3, the gas hourly space velocity (GHSV) was 40,000 h^{-1}. Catalytic experiments were carried out in a glass

Table 1

Content (wt.%)	
Co	Pd
–	–
0.57	–
–	0.48
0.58	0.63
0.57	0.14

Support: γ-Al_2O_3.

microreactor containing quartz wool supporting the sample. The bed temperature was measured using a K-type thermocouple affixed to the outer reactor surface. The temperature was controlled using an electronic controller (Eurotherm 2408).

The reactor outflow was analyzed using a set of specific detectors. An Eco Physics CLD 700 AL NO_x Chemiluminescence analyzer (for NO and total NO_x (i.e. $NO + NO_2$)) allowed the simultaneous detection of NO, NO_2 and NO_x. An Ultramat 6 IR analyzer was used to monitor N_2O and a FID detector was used to follow the total concentration of hydrocarbons (HC). Moreover, a mass spectrum (Hiden) was coupled to the experiment, at the outlet of the reactor, to monitor the following species: N_2 (amu = 28), O_2 (amu = 32), CH_3OH (amu = 31), HCHO (amu = 29), NO_2 (amu = 46) and Ar (amu = 40).

Temperature programmed desorption (TPD) experiments were carried out in Ar/O_2 (7 vol.% O_2 in Ar as balance, 0.250 L min^{-1}) with a heating rate of 5 °C min^{-1}, up to 500 °C, over pretreated samples. Before TPD gas mixture was pre-adsorbed (150 ppm NO, 7 vol.% O_2 in Ar as balance, 0.250 L min^{-1}).

Temperature programmed surface reaction (TPSR) experiments were carried out with all gases with a heating rate of 5 °C min^{-1}, up to 500 °C. Isothermal steady-state reaction was measured at different temperatures, ranging from 300 to 500 °C. The NO_x and methane conversions were calculated from measured concentration of NO_x and methane, respectively.

3. Results and discussion

3.1. Highly dispersed cationic materials

The materials, listed in Table 1, were characterized by XRD and no diffraction peaks of Co or Pd were detected. Furthermore no crystallized phases were found by HRTEM, although EDS showed that Pd/Al and Co/Al ratios were constant. Cobalt and palladium species were then highly dispersed on the support. Thus, UV–vis–NIR diffuse reflectance was performed to characterized theses latter species. The UV–vis–NIR diffuse reflectance spectra of Co(X)/Al_2O_3 and Pd(X)Co(X)/Al_2O_3 catalysts are displayed in Fig. 2. The spectra of the support consists mainly on several bands in the NIR due to: (i) ν_{OH} overtones of surface hydroxyl groups (1364 nm) and (ii) a combination of ν_{OH} and δ_{OH} (1885 and 2207 nm) [24]. After exchange of cobalt, the spectra showed a set of three bands at 540, 580, and 633 nm. As already reported in literature [25], these three bands are indicative of tetrahedral Co^{2+} ions, as found in the compound $CoAl_2O_4$. For Pd(X)Co(X)/Al_2O_3 catalyst a new band was observed at 420 nm, this band is characteristic of isolated Pd^{2+} in an oxygen environment [26]. As reported in Fig. 2, this band increases with the palladium content.

In conclusion, no particles of Co_3O_4 and PdO were detected. Moreover, in our samples, the cobalt and the palladium are in cationic form, Co^{2+} and Pd^{2+}, respectively, and well dispersed on the support.

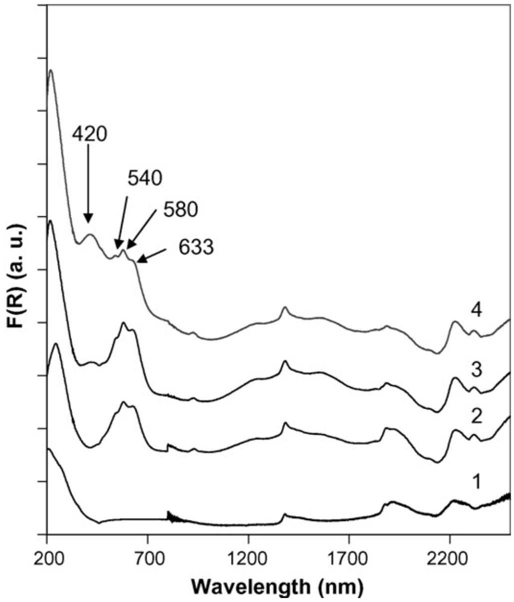

Fig. 2. UV–vis–NIR diffuse reflectance spectra of the Co(X)Pd(X)/Al_2O_3 catalysts—1: Al_2O_3; 2: Co(0.57$_2$O$_3$; 3: Co(0.57)Pd(0.14)/Al_2O_3; 4: Co(0.58)Pd(0.63)/Al_2O_3.

3.2. Prediction of NO_x temperature reduction

Fig. 3 shows the TPD of NO pre-adsorbed at room temperature on two different cobalt–palladium catalysts, Pd(0.63)Co(0.58)/Al_2O_3 (a) and Pd(0.14)Co(0.57)/Al_2O_3 (b), respectively. On cobalt–palladium catalysts, two desorption peaks of NO are observed (Fig. 3(a)-1 and (b)-1). For Pd(0.63)Co(0.58)/Al_2O_3, the two desorption peaks appear at 205 and 423 °C, whereas for Pd(0.14)Co(0.57)/Al_2O_3, the maxima desorption temperature peaks are at 205 and 487 °C. Thus, the second desorption peak depends on the catalyst formulation. Moreover, during the TPD, two NO_2 production peaks are observed at temperatures close to those observed for the NO desorption peaks (Fig. 3(a)-2 and 3(b)-2). These peaks can be attributed to the oxidation of adsorbed NO by palladium or cobalt species during the TPD in O_2/Ar (function 1 of the model [17,18]), or to the decomposition of nitrates adsorbed on the support (Fig. 3(c)-2). On each catalyst, the amount of high temperature NO_2 desorption is higher than that of NO.

On the support only one large NO desorption peak, below 500 °C, is observed (Fig. 3(c)-1). The maximum of this peak also appears in the range of temperature 200–250 °C. So, the first NO desorption peak, on bimetallic catalysts, can be attributed to the NO adsorbed on the support. A maximum of 40 ppm NO_2 was found at 485 °C. Park [27] showed that the NO_2 desorption was due to nitrate decomposition from the support, since alumina was not active for NO oxidation.

On the cobalt catalyst (Co(0.57)/Al_2O_3) (Fig. 4(a)-1 and -2), the results are quite similar to those obtained on the support alone. Again, only one large NO desorption peak is observed below 500 °C. The maximum of this peak is centred at 220 °C. A NO_2 desorption peak is observed at high temperature (Fig. 4(a)-2). This peak is larger than those obtained on the alumina. As already reported for Co–Pd catalysts, the NO_2

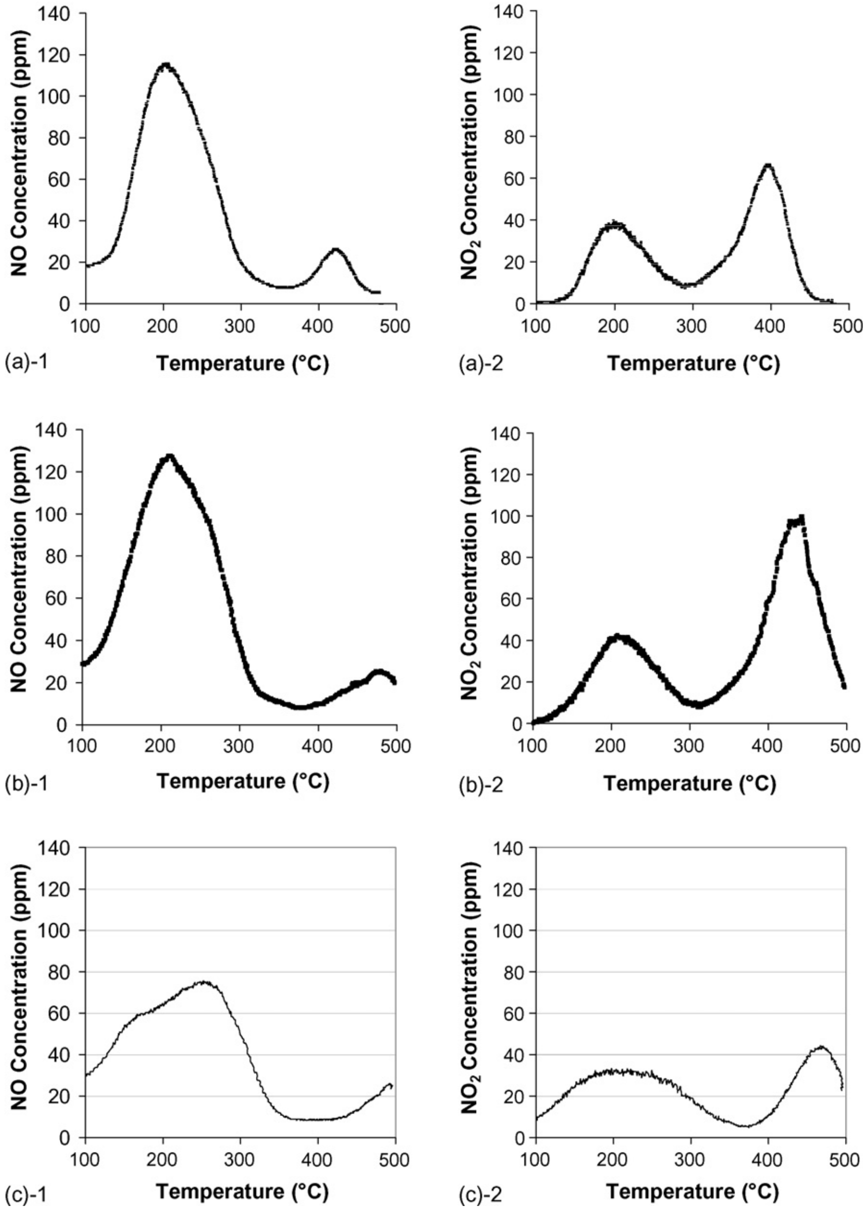

Fig. 3. Temperature programmed desorption (TPD) profiles of NO (1) and NO_2 (2) in Ar/O_2 (7 vol.% O_2, 5 °C min^{-1}, up to 500 °C) over: (a) Co(0.58 wt.%)Pd(0.63 wt.%)/Al_2O_3, (b) Co(0.57 wt.%)Pd(0.14 wt.%)/Al_2O_3, (c) Al_2O_3 (after a pre-adsorption at RT of NO–O_2 (150 ppm–7 vol.%), Ar as balance).

desorption could be attributed to the oxidation of adsorbed NO or to nitrate decomposition.

On the palladium catalyst (Pd(0.48)/Al_2O_3), presented in Fig. 4(b)-1 and -2, one can see that the results are quite similar to those obtained for the bimetallic catalyst Pd(0.63)Co(0.58)/Al_2O_3 (Fig. 3(a)-1 and -2). Two NO desorption peaks were found. Thus, we can conclude that the high NO desorption temperature peak can be attributed to the NO adsorbed on the palladium species. Furthermore, the maximum of the second desorption peak depends on the palladium content. According to Fig. 3(a)-1, (b)-1 and (c)-1, the second NO desorption peak is shifted to low temperatures with the increase of palladium content. These results confirm that the second peak of desorption is due to the NO adsorbed on palladium species. However, by UV–vis–NIR, we have shown that palladium is only present on the catalyst as Pd^{2+} surrounded by oxygen O^{2-} [26], and therefore, the second desorption peak is due to the NO adsorbed on Pd^{2+} species. Again, a large NO_2 desorption peak is observed at high temperature. A large amount of NO_2 during NO TPD in presence of O_2 has been already observed by Lobree et al. [28] on Pd–H–ZSM-5 catalysts. They had suggested that NO_2 could be formed by transformation of NO adsorbed. Thus, on palladium catalyst, the NO_2 desorption peaks could be attributed to the oxidation of the adsorbed NO by palladium species or to the decomposition of nitrates adsorbed on the support.

3.3. Catalytic performance of the cobalt–palladium catalysts

The deNO_x catalytic behaviour was studied in TPSR and in steady-state conditions. Before TPSR, the catalysts were

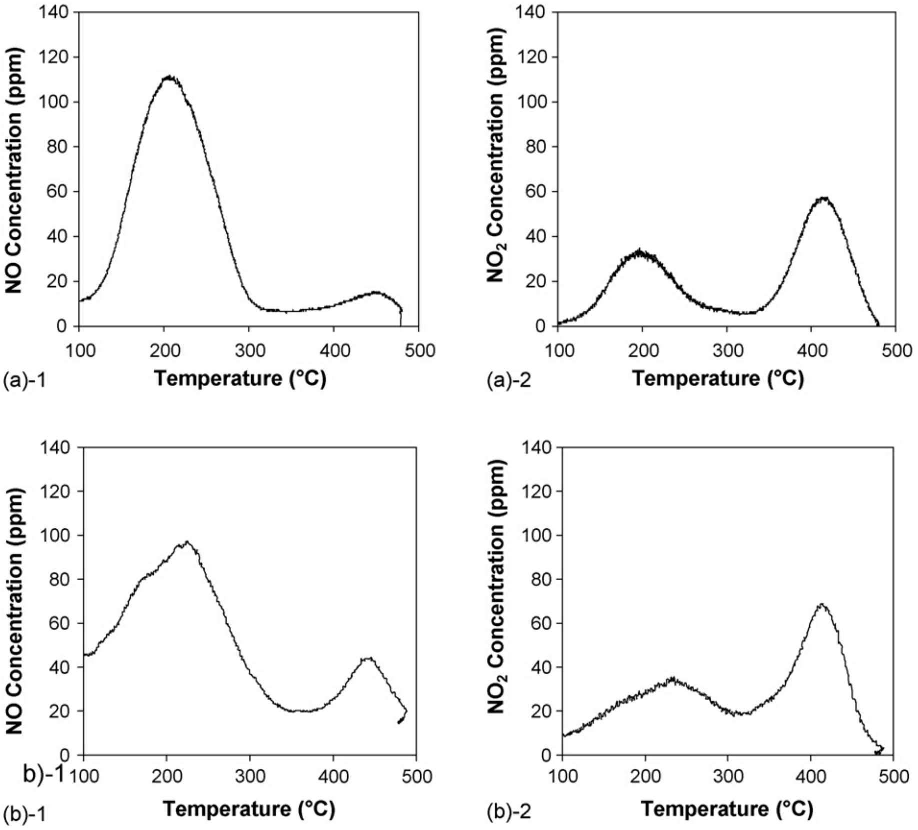

Fig. 4. Temperature programmed desorption (TPD) profiles of NO (1) and NO_2 (2) in Ar/O_2 (7 vol.% O_2, 5 °C min^{-1}, up to 500 °C) over: (a) Co(0.58 wt.%)/Al_2O_3, (b) Pd(0.5 wt.%)/Al_2O_3 (after a pre-adsorption at RT of NO–O_2 (150 ppm–7 vol.%), Ar as balance).

exposed to the reaction mixture at room temperature. The adsorption time was 1.25 h. The TPSR results are presented in Fig. 5 for Pd(0.63)Co(0.58)/Al_2O_3 (a), Pd(0.14)Co(0.57)/Al_2O_3 (b), Co(0.57)/Al_2O_3 (c) and Pd(0.48)/Al_2O_3 (d), respectively. For both catalysts, up to 250 °C, the observed features of NO and NO_2 are comparable to those obtained in TPD (Fig. 3).

Above 300 °C, a simultaneous consumption of methane and NO_2 is observed on Pd(0.63)Co(0.58)/Al_2O_3. This consumption is attributed to methane activation by NO_2, leading to a mild oxidation of methane. This reaction corresponds to the second function of the deNO$_x$ model proposed elsewhere [17–20]. Moreover, there is also a total oxidation of methane by O_2 leading to CO_2. The results are presented in Fig. 6. The methane light off temperatures are 340 and 360 °C for methane oxidation and deNO$_x$ reaction, respectively. Furthermore, at 500 °C, the methane oxidation is total, since 1500 ppm of CO_2 are detected. During the methane oxidation, no products from mild oxidation are detected. The same behavior is observed on the low loading Pd catalysts but at higher temperature, which is in agreement with the literature [19].

A deNO$_x$ activity is observed on both catalysts at different temperature window, 350–475 °C for Pd(0.63)Co(0.58)/Al_2O_3 and 425–500 °C for Pd(0.14)Co(0.57)/Al_2O_3. The activity is maximum (8% conversion of NO$_x$) at 410 °C and (13% conversion of NO$_x$) at 500 °C for Pd(0.63)Co(0.58)/Al_2O_3 and Pd(0.14)Co(0.57)/Al_2O_3, respectively. The reduction of NO$_x$ corresponds to the temperature window of the second NO desorption peak (Fig. 3(a)-1 and (b)-1).

On the support alone, no deNO$_x$ activity nor methane consumption are observed in the studied temperature range (100–500 °C). On cobalt Co(0.57)/Al_2O_3 and Pd(0.48)/Al_2O_3, no deNO$_x$ activity is observed from 350 to 475 °C (Fig. 5(c) and (d)). For the cobalt catalyst, the NO_2 consumption at high temperatures (300–500 °C) is very low, and the methane is only transformed at temperatures higher than 350 °C. On the cobalt catalyst, the methane activation by NO_2 is very low, and the major consumption of methane leads directly to CO_2 due to the total oxidation of methane by O_2. On the palladium catalyst, at high temperatures, no NO_2 feature was observed. In the same range of temperatures methane was consumed. A part of the methane reacts with the NO_2 leading to NO and oxygenated species of methane (function 2 of the catalyst [17–20]). The other part is totally oxidized to CO_2, being the total oxidation favoured at high temperatures [29].

The deNO$_x$ temperature window is confirmed for both bimetallic catalysts in steady-state conditions. Indeed, as reported in Fig. 7(a) and (b), more than 5% NO$_x$ conversion is obtained between 350 and 450 °C, for Pd(0.63)Co(0.58)/Al_2O_3, and between 410 and 500 °C, for Pd(0.14)Co(0.57)/Al_2O_3. These high temperatures conversion are only attributed to the reduction of NO$_x$ to N_2, as reported in the literature on alumina supported materials [27]. Indeed,

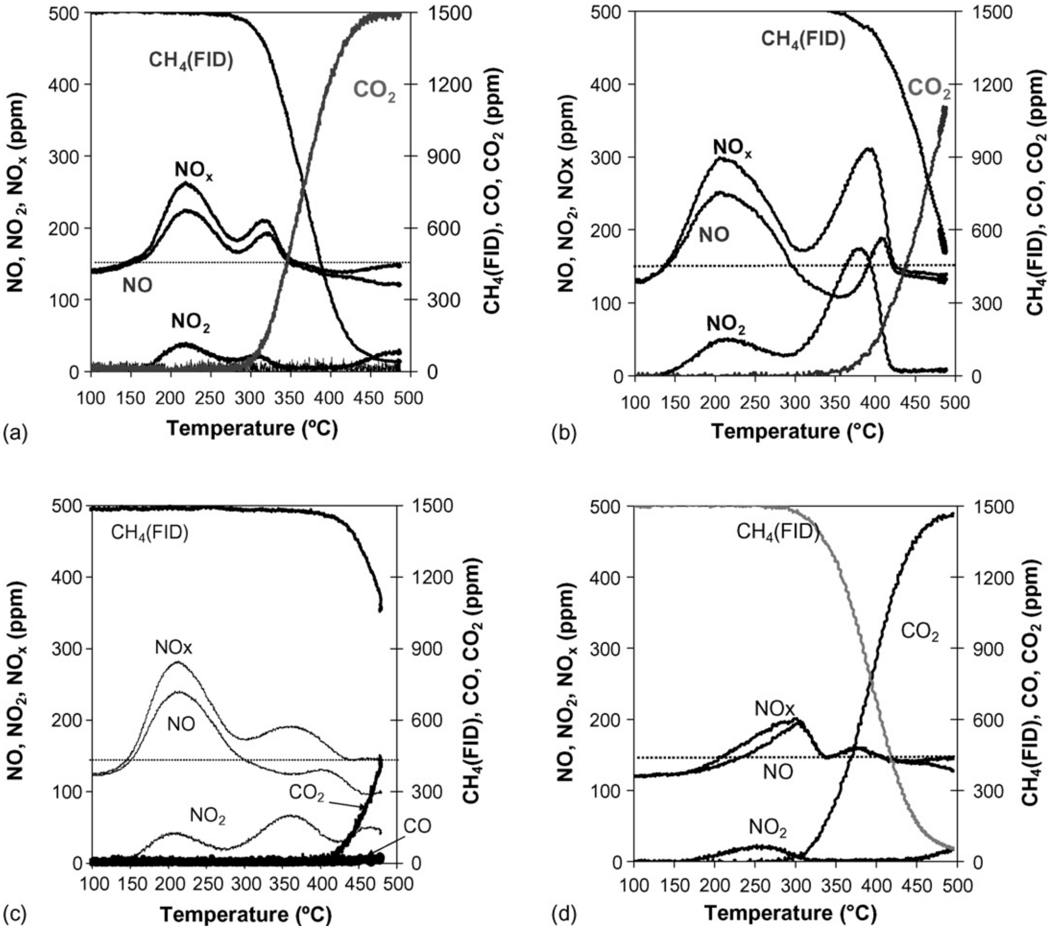

Fig. 5. Temperature programmed surface reaction profiles (TPSR) with CH_4–NO–O_2 (1500 ppm–150 ppm–7 vol.%), Ar as balance over: (a) Co(0.58 wt.%)Pd(0.63 wt.%)/Al_2O_3, (b) Co(0.57 wt.%)Pd(0.14 wt.%)/Al_2O_3, (c) Co(0.57 wt.%)/Al_2O_3, (d) Pd(0.47 wt.%)/Al_2O_3.

nitrogen ($m/z = 28$) is detected by mass spectroscopy (Hiden) from 350 to 500 °C over Pd(0.63)Co(0.58)/Al_2O_3 (Fig. 8).

As comparison, the support, the cobalt and the palladium catalysts were tested in the same isothermal conditions. On the support alone, and on Co(0.57)/Al_2O_3, no deNO$_x$ activity has been observed. On the palladium catalyst Pd(0.48)/Al_2O_3, only 6.5% deNO$_x$ conversion to N_2 was obtained at 390 °C in steady-state conditions (Fig. 9).

Hence, there is a synergetic effect between the cobalt and the palladium leading to a high reactivity of bimetallic catalyst Pd(0.63)Co(0.58)/Al_2O_3 on a large temperature window.

3.4. deNO$_x$ mechanism over the cobalt–palladium catalysts for stationary sources

As already reported in the literature [17–22], a three function lean deNO$_x$ mechanism can be used on zeolite and ceria–

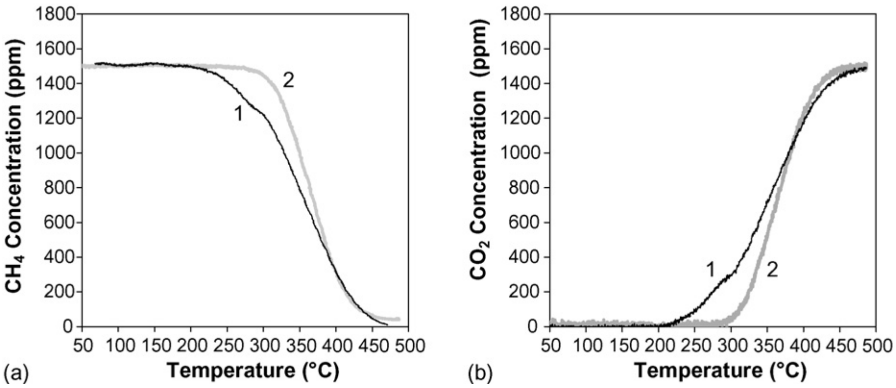

Fig. 6. (a) Evolution of the methane concentration; (b) evolution of the CO_2 concentration; in the course of TPSR of (1) CH_4 (1500 ppm), O_2 7%, Ar as balance (methane oxidation) and (2) CH_4 (1500 ppm), NO (150 ppm), O_2 7%, Ar as balance (deNO$_x$ reaction) over Co(0.58 wt.%)Pd(0.63 wt.%)/Al_2O_3.

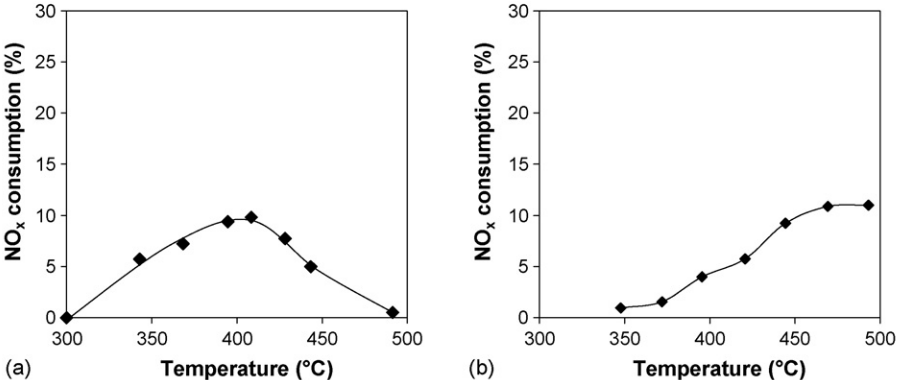

Fig. 7. Isothermal steady-state consumption of NO_x in the course of CH_4–NO–O_2 (1500 ppm–150 ppm–7 vol.%), Ar as balance over: (a) Co(0.58 wt.%)Pd(0.63 wt.%)/Al_2O_3, (b) Co(0.57 wt.%)Pd(0.14 wt.%)/Al_2O_3.

zirconia supported cations (Co, Pd). From the presented results, on alumina supported Co–Pd catalysts, the deNO$_x$ catalytic activity can be explained by the three function model.

In the three function model, the first function is the NO oxidation in NO_2. On Co(0.58 wt.%)Pd(0.63 wt.%)/Al_2O_3 catalyst, and for temperature window, in which the deNO$_x$ reaction takes place, one can see that the NO oxidation is not negligible. A 57 ppm of NO_2 were observed at 400 °C (Fig. 10). The NO oxidation can take place on cobalt and palladium species.

The second function is the methane activation by NO_2, leading to NO and oxygenate species, which are the ‘‘real’’ reductants for deNO$_x$ reaction [22]. On Co(0.58 wt.%)Pd (0.63 wt.%)/Al_2O_3 catalyst, the NO_2 concentration detected during the TPSR are shown in Fig. 10, where one can see that no NO_2 is detected at temperatures lower than 425 °C. The absence of NO_2 in the course of the TPSR indicated that the NO_2 produced by the first function, reacted. According to the general deNO$_x$ model presented in Fig. 1, methane should be activated by NO_2, in a mild oxidation, to form oxygenate species, such as alcohols and aldehydes [17,18]. Thus, we tried to follow the intermediate of the reaction by mass spectroscopy (MS). In our experiments, in the course of steady-state reaction, the only intermediate species detected was the formaldehyde (HCHO) (Fig. 11). This kind of intermediate has been already reported on zeolites materials for SCR deNO$_x$ by methane [24]. The second function was then demonstrated on alumina supported Co–Pd catalysts. As one can see in Fig. 5(a) for Co(0.58 wt.%)Pd(0.63 wt.%)/Al_2O_3 and in Fig. 5(d) for Pd(0.48 wt.%)/Al_2O_3, the same trends in NO_2 and CH_4 concentration are observed. No NO_2 is observed from 350 to 440 °C, and methane is consumed from 300 °C. On the other hand, for the cobalt catalyst (Fig. 5(c)), the methane is only consumed until 350 °C and the NO_2 is observed in the range where there is deNO$_x$ activity. These observations lead us to conclude that the methane activation is done on the palladium species, Pd^{2+} surrounded by the oxygen detected by UV–vis–NIR [26].

The third function is the NO decomposition assisted by ‘‘oxygenated species’’ [18–20] leading to N_2. According to Fig. 8, dinitrogen is detected during the isothermal reactions (Fig. 7(a)) on the Co(0.58 wt.%)Pd(0.63 wt.%)/Al_2O_3 catalyst.

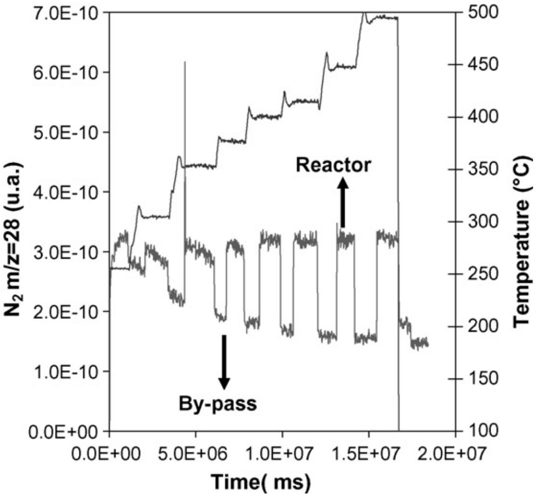

Fig. 8. Mass spectra of the nitrogen (amu = 28) over Co(0.58 wt.%)Pd (0.63 wt.%)/Al_2O_3 in the course of CH_4–NO–O_2 (1500 ppm–150 ppm–7 vol.%), Ar in steady state conditions.

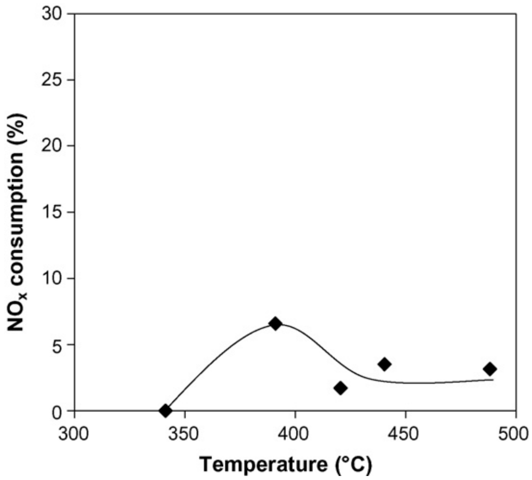

Fig. 9. Isothermal steady-state consumption of NO_x in the course of CH_4–NO–O_2 (1500 ppm–150 ppm–7 vol.%), Ar as balance over: Pd(0.63 wt.%)/Al_2O_3.

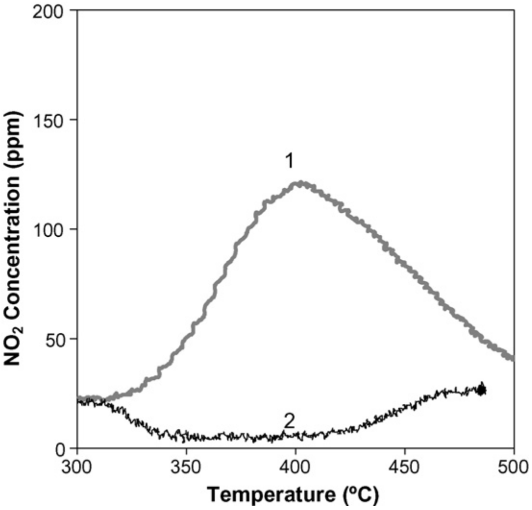

Fig. 10. Evolution of the NO_2 concentration; in the course of TPSR of (1) NO (150 ppm), O_2 7%, Ar as balance (NO oxidation) and (2) CH_4 (1500 ppm), NO (150 ppm), O_2 7%, Ar as balance (deNO_x reaction) over Co(0.58 wt.%)Pd (0.63 wt.%)/Al_2O_3.

In the same temperature range, NO_2 reacted with methane leading to NO and ‘‘oxygenate species’’. These latter species then reacted then with NO originating N_2, CO_2 and H_2O. It was proposed that this third function was done on metallic sites in the cationic form [17,20,27]. Park [27] has recently shown that alumina supported cobalt catalysts are active catalysts for SCR deNO_x by methanol, leading to 100% deNOx activity up to 400 °C. On the Pd(0.48 wt.%)/Al_2O_3 catalyst, we also followed the intermediate species and the dinitrogen, by MS, during the isothermal steady state experiments. Similar results to those obtained for the Co(0.58 wt.%)Pd(0.63 wt.%)/Al_2O_3 catalyst were reached. HCHO was found in the course of the deNO_x reaction in the range where the deNO_x conversion into N_2 is observed. Thus, the third function is done also on Pd^{2+} species. By UV–vis–NIR, on bimetallic catalysts, the palladium and the cobalt have been found as Pd^{2+}, in oxygen environment, and Co^{2+}, respectively. Thus, the third function can be performed on both sites [21]. As a result, on the bimetallic catalysts, the deNO_x activity is higher than on the metallic ones, due to the increase of active sites for the three functions of deNO_x mechanism.

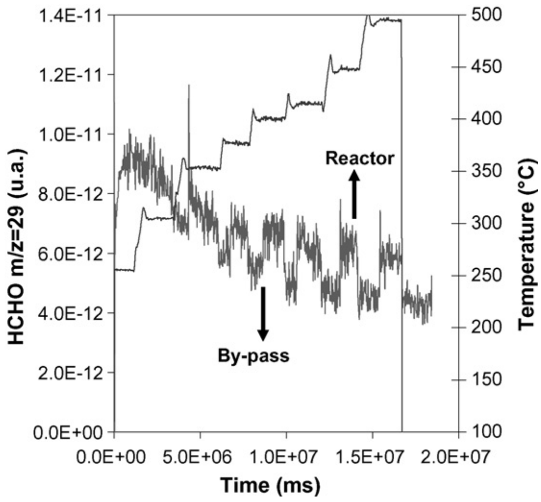

Fig. 11. Mass spectra of the reaction intermediates: HCHO (amu = 31) over Co(0.58 wt.%)Pd(0.63 wt.%)/Al_2O_3 in the course of CH_4–NO–O_2 (1500 ppm–150 ppm–7 vol.%), Ar in steady state conditions.

4. Conclusions

Alumina supported cobalt–palladium catalysts were tested for NO reduction by methane, in a representative mixture of exhausted gases of CHP in the absence of water. By UV–vis–NIR, we have shown that both cobalt and palladium are in the cationic form, Co^{2+} and Pd^{2+}, respectively.

Isothermal steady-state reaction from 300 to 500 °C was performed and moderated activity in deNO_x reduction was found. Using a GHSV of 40,000 h^{-1}, the activity is maximal (8% conversion of NO_x) at 410 °C and (13% conversion of NO_x) at 500 °C for Pd(0.63)Co(0.58)/Al_2O_3 and Pd(0.14)Co(0.57)/Al_2O_3, respectively. The second NO desorption peak corresponds to the temperature window of the reduction of NO (deNO_x) during the TPSR. This second desorption peak can be attributed to NO adsorbed on Pd^{2+} species, which indicates that the third function of the general deNO_x model can take place on the Pd^{2+} sites. Moreover, the second function (methane activation by NO_2) of the ‘‘three function’’ model proposed was also demonstrated on our catalysts. Indeed, NO_2 is not detected at high temperatures during the TPSR experiments. NO_2 reacted with methane to form oxygenate species, since formaldehyde was detected in the steady state isothermal reaction at the same temperature range of deNO_x activity. The methane activation is favoured by the Pd^{2+} species.

As conclusion, on the studied catalysts, the three catalytic cycles (‘‘tree function model’’) have turned simultaneously:

(1) oxidation of NO into NO_2, on the cobalt and the palladium species,
(2) mild oxidation of methane ($CH_4 + NO_2 \rightarrow C_xH_yO_z$), on the palladium species,
(3) reduction of NO with total oxidation of $C_xH_yO_z$ species, on the cobalt and the palladium species.

Acknowledgements

This work was carried out in the framework of the European program ‘‘EUREKA’’ STATIONOCAT. Rui Marques acknowledges the financial support of ADEME and Gaz de France in the form of an ‘‘ADEME’’ grant. Prof. Bozon-Verduraz and Ing. F. Warmont are greatly acknowledged for UV–vis and TEM experiments, respectively.

References

[1] Y. Li, J. Armor, J. Catal. 150 (1994) 376.
[2] L.F. Cordoba, G.A. Fuentes, C. Montes de Correa, Micropor. Mesopor. Mater. 77 (2005) 193.
[3] F. Bustamante, F. Córdoba, M. Yates, C. Montes de Correa, Appl. Catal. A 234 (2002) 127.
[4] M. Ogura, Y. Sugiura, M. Hayashi, E. Kikuchi, Catal. Lett. 42 (1996) 185.

[5] M. Ogura, S. Kage, T. Shimojo, J. Oba, M. Hayashi, M. Matsukata, E. Kikuchi, J. Catal. 211 (2002) 75.
[6] M. Iwamoto, H. Yahiro, Catal. Today 22 (1994) 5.
[7] M. Iwamoto, H. Hamada, Catal. Today 10 (1991) 57.
[8] C.J. Loughran, D.E. Resasco, Appl. Catal. B Environ. 7 (1995) 113.
[9] Y.–H. Chin, A. Pisanu, L. Serventi, W.E. Alvarez, D.E. Resasco, Catal. Today 54 (1999) 419.
[10] L.F. Córdoba, W.M.H. Sachtler, C.M. Correa, Appl. Catal. B 56 (2005) 569.
[11] N. Li, A. Wang, L. Ren, M. Zheng, X. Wang, T. Zhang, Topics Catal. 30/31 (2004) 103.
[12] N. Li, A. Wang, M. Zheng, X. Wang, R. Cheng, T. Zhang, J. Catal. 225 (2005) 307.
[13] J.A.Z. Pieterse, R.W. van den Brink, S. Booneveld, F.A. de Bruijn, Appl. Catal. B 39 (2002) 167.
[14] J.A.Z. Pieterse, R.W. van den Brink, S. Booneveld, F.A. de Bruijn, Appl. Catal. B 46 (2003) 239.
[15] R. Burch, J.P. Breen, F.C. Meunier, Appl. Catal. B 39 (2002) 283.
[16] V.I. Pârvulescu, P. Grange, B. Delmon, Catal. Today 46 (1998) 233.
[17] G. Djéga-Mariadassou, M. Boudart, J. Catal. 216 (2003) 89.
[18] G. Djéga-Mariadassou, Catal. Today 90 (2004) 27.
[19] C. Thomas, O. Gorce, C. Fontaine, J.-M. Krafft, F. Villain, G. Djéga-Mariadassou, Appl. Catal. B 63 (2006) 201.
[20] A.P. Ferreira, S. Capela, P. Da Costa, C. Henriques, M.F. Ribeiro, F.R. Ribeiro, Catal Today, in press.
[21] M. Berger, PhD Thesis, Université P. & M. Curie, Paris, France, 2000.
[22] F. Baudin, P. Da Costa, C. Thomas, S. Calvo, Y. Lendresse, S. Schneider, F. Delacroix, G. Plassat, G. Djéga-Mariadassou, Topics Catal. 30/31 (2004) 97.
[23] P. Gélin, L. Urfels, M. Primet, E. Tena, Catal. Today 83 (2003) 45.
[24] K. Elkabouss, M. Kacimi, M. Ziyad, S. Ammar, F. Bozon-Verduraz, J. Catal. 226 (2004) 16.
[25] J. Yan, M.C. Kung, W.M.H. Sachtler, H.H. Kung, J. Catal. 172 (1997) 178.
[26] D. Tessier, A. Rakai, F. Bozon-Verduraz, J. Chem. Soc. Faraday Trans. 88 (1992) 741.
[27] J.W. Park, PhD Thesis, Université P. & M. Curie, Paris, France, 2005.
[28] L.J. Lobree, A.W. Aylor, J.A. Reimer, A. Bell, J. Catal. 181 (1999) 189.
[29] J. Haber, W. Turek, J. Catal. 190 (2000) 320.